ELSEVIER

Clinical Biomechanics Vol. 12, No. 7/8, pp. 461–472, 1997

Printed in Great Britain
0268-0033/97 $17.00 + 0.00

PII: S0268-0033(97)00031-4

The variability of shoulder motions recorded by means of palpation

Jurriaan H de Groot

Laboratory of Measurement and Control, Faculty of Mechanical Engineering and Marine Technology, Delft University of Technology, Delft, The Netherlands

Abstract

Objective. The objective of this methodological study is the quantification of the sources of variability in the recorded three-dimensional motions of the shoulder mechanism for comparative purposes.
Background. The palpation and subsequent digitization of skeletal landmarks of the shoulder mechanism is a non-invasive and relatively easy method to quantify shoulder orientations. Comparison of individual motions is subject to the accuracy of the palpation method, the magnitude of kinematic redundancy of the shoulder mechanism and inter-subject differences in morphology and physiology. Quantification of these sources of variance, i.e. the palpation error, motoric noise and inter-subject differences, demonstrated the accuracy of the method and the potential validity of the descriptive motion parameters, e.g. Cardan angles, in intra- and inter-individual studies for clinical, ergonomical and biomechanical studies.
Methods. The orientations of the shoulder bones were recorded five times for each of five subjects by palpation and digitization of 12 skeletal landmarks for 10 equidistant arm elevation postures in the scapular plane. The orientations were described by means of Cardan angles. The palpation error was determined at a standardized initial rest position and expressed by Cardan angles for each recorded posture. Adding motoric noise and inter-subject differences gave the inter-individual variance.
Results. The palpation error was approximately 2°. The major recorded variance originated from motoric noise (±33%) and inter-subject difference (±55%).
Conclusions. The palpation method is an accurate means of recording the three-dimensional orientations of the shoulder mechanism and for intra-individual studies. However, inter-subject variability is large.

Relevance

The parameters describing shoulder orientations are essential for biomechanical analysis by means of musculoskeletal shoulder models, and supply descriptive parameters for the comparative analysis and follow-up of individual shoulder motions in clinical and ergonomic settings, e.g. glenohumeral immobility and impingement.

Key words: Shoulder, kinematics, palpation method, variance

Clin. Biomech. Vol 12, No. 7/8, 461–472 1997

Introduction

The measurement and description of shoulder kinematics are important features in understanding and solving the causes of shoulder complaints and related problems in both the clinical setting, e.g. glenohumeral (GH) dislocation, impingement, frozen shoulder, and the ergonomic setting, e.g. job-related shoulder complaints and the efficiency of arm-propelled wheelchairs. Both the measurement and description of the movements of the shoulder have their particular problems.

Three-dimensional (3D) recording is only possible by means of bi-planar Roentgen photogrammetry[1] or percutaneous pins[2], both of which are invasive methods, or by means of the digitization of the spatial coordinates of palpated skeletal landmarks[3–7]. Although palpation is a static method to record the position of the skeletal bones, the kinematics of the

Correspondence and reprint requests to: J H de Groot. Tel: +31 15 2782156; Fax: +31 15 2784717; E-mail: J.H.DeGroot@wbmt.tudelft.nl

movement can be determined by means of interpolation of the postures. By means of planar Roentgen video of arm abduction[8] it can be shown that movement velocity only negligibly affects the kinematics of the scapulohumeral rhythm.

The movement of the shoulder mechanism is described by the spatial movement of the thorax, the clavicula, the scapula and the humerus, respectively. This movement is expressed by three Cardan angles for each of the bones[7]. A disadvantage of using Cardan angles is the order dependency of the three angles, and the increasing inaccuracy at positions near the singular position 'gimbal-lock' position. These negative effects can be minimized by an appropriate choice of the local coordinate systems and rotation order.

As a result of the degrees of freedom of the shoulder mechanism and the differences between subjects (e.g. morphological, physiological) none of the arm–shoulder movements will be equal. The measured intra-individual variance and inter-individual variance is caused by three sources of variability, which are considered to be independent and can be identified by:

- The palpation error (E_P): the inaccuracy in determining the exact spatial position of a skeletal landmark by means of palpation and digitization.
- The motoric noise (E_M): the kinematic variability of positioning of the shoulder bones resulting in the same arm position and originating from different muscle force distributions.
- The inter-subject differences (E_S): the differences between shoulder kinematics due to the different morphologies, muscle strength and motor strategies in the subject population.

The inter-individual variance of the shoulder orientations for a population of subjects is determined by the summed effects of E_P, E_M, and E_S. The intra-individual variance of the shoulder orientations is determined by the summed effects of E_P and E_M.
The goal of this work is to quantify the independent sources of variability and to evaluate the obtained rotational parameters for clinical and ergonomic applications.

Methods

Experiment

An arm abduction was performed by $N_S = 5$ healthy male subjects (aged 26 ± 2 years). The recordings of the kinematics were made at $N_P = 10$ static positions in the scapular plane, 30° with the frontal plane in a random order and with arm abduction positions: minimal abduction, 20°, 40°, ..., 160°, maximal abduction. The elbow was flexed to 90° and the lower arm was kept in the plane of arm abduction. The position of the subjects was standardized by establishing fixed positions of the head, the hips and the feet (Figure 1). Each set of 10 postures was measured $N_R = 5$ times.

Recording

The kinematics of the shoulder mechanism were recorded by means of palpation and 3D digitization[3,7]. Palpable skeletal landmarks were identified on each of the shoulder bones (Table 1). The spatial position of the landmarks during the trials was localized by palpation and was subsequently digitized with a 3D pointer, the palpator[4], with a root mean square error of 0.1 mm.

Before movement registration the morphology, i.e. the geometrical relationships of the skeletal landmarks within the bones of the shoulder mechanism, was determined from $N_I = 5$ initial

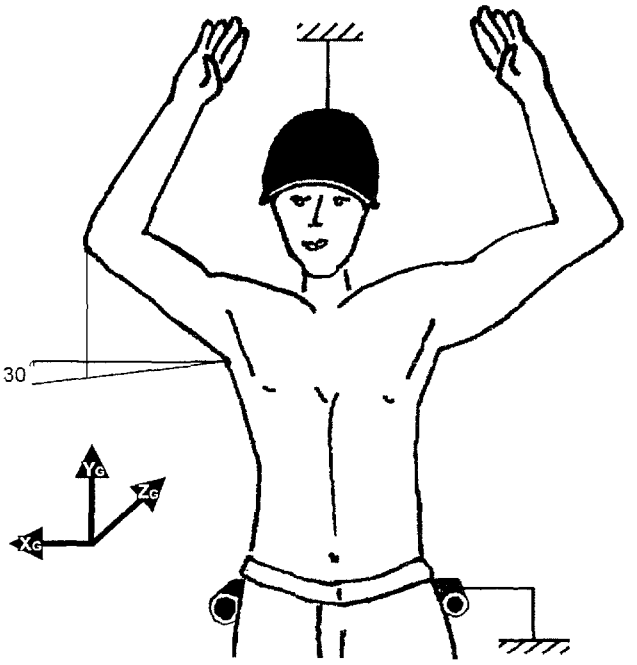

Figure 1. Schematic position of the subject with standardized positions of the head (fixed by a helmet), the hips (fixed by a U-shaped clamp) and the feet. The arm abduction plane was 30° rotated from the frontal plane, the elbows were flexed to 90°.

Table 1. Skeletal landmarks used to define the global orientation of the bones of the shoulder mechanism

Thorax	Clavicula	Scapula	Humerus
Incisura jugularis (IJ)	Sternoclavicular joint (SC)	Acromioclavicular joint (AC)	Epicondylus medialis (EM)
Processus xyphoideus (PX)	Acromioclavicular joint (AC)	Angulus acromialis (AA)	Epicondylus lateralis (EL)
Seventh cervical spine (C7)		Trigonum spinae (TS)	Glenohumeral joint (GH)
Eighth thoracic spine (T8)		Angulus inferior (AI)	

recordings of the subject in a rest position with the upper-arms vertical along the body and the elbow flexed to 90° forward. This subject-specific rigid-body morphology was used during the abduction recordings, in order to check the recorded positions of the skeletal landmarks. Deviations larger than 11 mm were identified as measurement errors and were subsequently remeasured.

Glenohumeral reconstruction

All landmarks in Table 1, except the GH joint, can be palpated. As the shape of the glenoid and the articular surface of the humerus are almost congruent spheres[9,10] the position of the rotation centre defined on the humerus is equal to the position of the rotation centre on the scapula. Based on this principle the regression equation from four scapular bony landmarks was determined to deduce the position of the GH rotation centre from 14 shoulder specimens[11]. These equations were used to calculate the position of the GH centre of rotation (see Appendix).

Local coordinate systems

The right-handed coordinate systems were defined according to Figure 2. The orientation of the global coordinate system (G_G, Y_G, Z_D) is defined by means of external markers determining a horizontal and vertical axis, parallel to the frontal plane of the subjects. The origin is fixed at the thorax (incisura jugularis; IJ). The local coordinate systems of the shoulder bones are defined according to Table 2. For the scapula two different local coordinate systems were compared. The results presented are based on the local coordinate system using the skeletal landmarks angulus acromialis (AA), trigonum spinae (TS) and angulus inferior (AI)[3,5,12]. The results have been compared with the rotations calculated using the skeletal landmarks acromioclavicular joint (AC), TS and AI[6,7].

Cardan rotations

Rotations were calculated relative to the global coordinate system. In order to be able to compare the positions of different measurements, a unique reference position was defined. Either of two reference postures could be chosen:

- The average initial posture of the abduction movement[3,5], with the hands along the body. All calculated rotations will start from 0°. Relative positions are presented.
- A virtual anatomical posture with the local coordinate systems aligned with the global coordinate system[6]. The calculated rotations start with an offset value. The absolute orientation of the shoulder bones is given.

The latter option, which is independent of the subject's/patient's ability to realize this position, was applied. The local position matrices of the shoulder bones, representing the orientation of the coordinate systems with respect to the reference system, were decomposed into Cardan angles[3,6,13]. The order of decomposition is presented in Table 3.

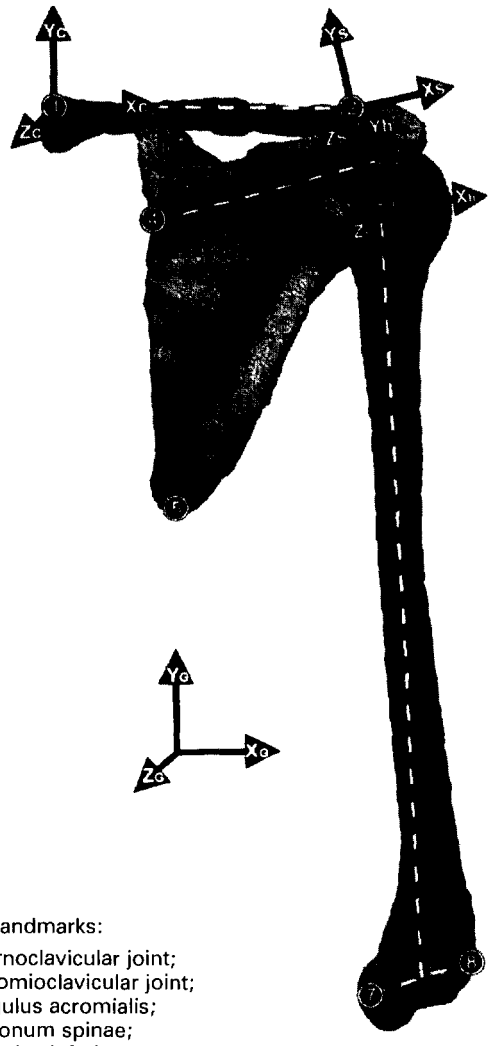

Bony landmarks:

1. sternoclavicular joint;
2. acromioclavicular joint;
3. angulus acromialis;
4. trigonum spinae;
5. angulus inferior;
6. glenohumeral joint;
7. medial epicondyle;
8. lateral condyle;

Coordinate systems (according to Table 2) with respect to the global coordinate system (X_G, Y_G, Z_G).
Clavicle:

(X_C, Y_C, Z_C)
origin: sternoclavicular joint.

Scapula:

(X_S, Y_S, Z_S)
origin: acromioclavicular joint.

Humerus:

(X_H, Y_H, Z_H)
origin: glenohumeral joint.

Figure 2.

Table 2. Definition of the local and global axes of the shoulder mechanism

Global	Origin: incisura jugularis
	X_G-axis: horizontally to the right
	Y_G-axis: vertically upward
	Z_G-axis: horizontally backward
Thorax	Origin: incisure jugularis
	X_T-axis: ⊥ on plane (IJ,PX,C7)
	Y_T-axis: (IJ–PX)/‖(IJ–PX)‖
	Z_T-axis: ⊥ on plane (X_T,Y_T)
Clavicula[a]	Origin: sternoclavicular joint
	X_C-axis: (AC–SC)/‖(AC–SC)‖
	Y_C-axis: ⊥ on plane (X_C,Z_C)
	Z_C-axis: ⊥ on plane (X_C,Y_G)
Scapula	Origin: acromioclavicular joint
	X_S-axis: (AA–TS)/‖(AA–TS)‖
	Y_S-axis: ⊥ on plane (X_S,Z_S)
	Z_S-axis: ⊥ on plane (AA,TS,AI)
Humerus	Origin: glenohumeral joint
	X_H-axis: ⊥ on plane (Y_H,Z_H)
	Y_H-axis: (GH–EP)/‖(GH–EP)‖ with $EP = (E_m+E_L)/2$
	Z_H-axis: ⊥ on plane (GH,E_m,E_L)

On the scapula only two landmarks can be found (SC and AC). Initially the global Y_G-axis is used to define the Y_C-axis and Z_C-axis. Pronk (1991)[3] estimated the axial rotation of the clavicula by minimization of the rotations at the AC joint.

Error differentiation

In the introduction three different sources of variance were defined: the palpation error E_P, the motoric noise E_M and the inter-subject differences E_S. The error of the digitizer (rms 0.1 mm) is negligibly small with respect to the accuracy of the palpation (critical distance: 11 mm between skeletal landmarks of the same bone). The errors were expressed as standard deviations of the Cardan angles that describe the motions of the shoulder mechanism.

The E_P describes the accuracy of the palpation method. It is determined by the shape of the skeletal landmarks and the tissue between the landmarks and the skin. In the optimal situation the E_P is estimated by repeated measurements of fixed bones. *In vivo* the position of the bones can only be standardized. $N_I = 5$ initial measurements were used to estimate the morphology of the subjects and to estimate the palpation error E_P. In order to minimize the effects of movements between the five different recordings, the centroid (centre of the skeletal landmarks) of the skeletal landmarks belonging to a specific bone was subtracted from each of the individual landmarks. The variance on the coordinates of each of the landmarks was estimated and expressed in the local coordinate systems of the bones.

For each bone except the clavicle, three landmarks have been used to calculate the position matrix (Table 2). The Cardan angles were determined susbsequently, and the position of each bone expressed in Cardan angles $X(\alpha, \beta, \gamma)$ is a function of the three coordinates (q) of each of the three landmarks (Eq. 1). The axial rotation was calculated by minimization of the rotations in the AC[3,6].

$$(\alpha,\beta,\gamma) = f(q_i), \text{ for } i = 1, 2, \ldots, 9. \quad (1)$$

Likewise the variance of the positions of the bones σ_x^2 is a function of the variance of each of the nine coordinates (σ_q^2). The function of variance can be approximated by using a first-order Taylor series expansion[14,15], assuming that the errors on the coordinates are independent and hence the co-variates are zero[6]:

$$\sigma_x^2 = \sum_{i=1}^{9} \left\{ \left(\frac{\partial f}{\partial q_i} \right)^2 \times \sigma_{q_i}^2 \right\}. \quad (2)$$

The E_P for the scapula, for example, is equal to σ_x estimated for the scapula from the variance on the coordinates of the skeletal landmarks of the scapula. The squared independent quantities E_p and E_m add up to the intra-individual variance (σ_{intra}^2):

$$\sigma_{\text{intra}}^2 = E_P^2 + E_M^2. \quad (3)$$

The intra-individual variance was obtained from $N_R = 5$ repeated measurements of $N_P = 10$ positions of the abduction movement. By subtracting the squared E_P from the intra-individual variance the squared motoric noise E_M was estimated.

Similarly, the squared quantities E_P, E_M and E_S add up to the inter-individual variance (σ_{inter}^2):

$$\sigma_{\text{inter}}^2 = E_P^2 + E_M^2 + E_S^2. \quad (4)$$

The inter-individual variance was obtained from $N_R \times N_P = 50$ positions for $N_S = 5$ subjects. By subtraction of the intra-individual variance from the inter-individual variance, the squared inter-subject difference E_S was identified.

The derivation of three Cardan angles from a rotation matrix is a non-linear operation. The accuracy of the Cardan parameterization is not constant over the range of arm abduction, e.g. the gimbal-lock position is ill-defined. Therefore, the variances of the 3D kinematics were estimated over

Table 3. Definition of the rotation order and the nomenclature of the rotations

Bone	Euler decomposition order			Rotation description		
Thorax	X	Y'	Z''	Backward rotation	Torsion	Lateral rotation
Clavicula	Y	Z'	(X'')	Protraction	Elevation	(Axial rotation)
Scapula	Y	Z'	X''	Protraction	Latero-rotation	Spinal tilt
Humerus	Y	Z'	Y''	Abduction plane	Abduction	Axial rotation

four intervals of 45° arm abduction: 1: (0–45°); 2: (45–90°); 3: (90–135°); 4: (135–180°).

Results

Initial measurements

The individual initial measurements served two purposes: the definition of the average morphology (geometry) was used as a reference during the rigid-body check after each measurement, and the measurements were used to determine the standard deviation σ_q of the coordinates of the bony landmarks in order to calculate the palpation error, Equation 2.

From $N_I = 5$ initial measurements the morphology of the subjects was determined (Table 4).

The exact identification of the position of the landmarks by means of palpation is not possible. In order to estimate the standard deviation on the coordinates the position of each of the shoulder bones was modelled as fixed by subtracting the centroid (centre of the skeletal landmarks) from the individual landmarks. The standard deviations of the landmarks σ_q were expressed in the local coordinate systems of the shoulder bones (Table 4).

Intra-individual variability

The orientations of the shoulder mechanism were estimated by a fifth-order polynomial least squares fit on the ($N_R \times N_p =$) 50 individual position recordings (Figure 3). The intra-individual variance σ^2_{intra} was estimated on the difference between the estimated and measured data for each of the four intervals of abduction.

Inter-individual variability

Similar to the intra-individual variation, the inter-individual variation was calculated for ($N_R \times N_p \times N_S =$) 250 position recordings (Figure 4).

Table 4. The average 3D positions (x, y, z) of the skeletal landmarks (mm) in the global coordinate system configured according to the anatomical reference system and the standard deviation σ_q on the coordinates in the local coordinate system

Skeletal landmark	X (mm)	Y (mm)	Z (mm)
IJ	0 ± (1.4)	0 ± (1.6)	0 ± (1.9)
PX	0 ± (2.1)	−169 ± (1.6)	0 ± (2.2)
SC	21 ± (2.0)	2 ± (1.9)	−0 ± (2.9)
C7	0 ± (2.3)	98 ± (3.3)	89 ± (1.9)
T8	1 ± (1.3)	−84 ± (1.2)	194 ± (3.1)
AC[a]	200 ± (2.3)	2 ± (1.0)	−0 ± (2.7)
AA	209 ± (2.9)	−28 ± (1.6)	27 ± (3.2)
TS	73 ± (3.8)	−34 ± (2.0)	27 ± (2.5)
AI	73 ± (3.8)	−149 ± (1.8)	27 ± (3.0)
GH	204 ± (3.5)	−39 ± (2.1)	−19 ± (3.3)
Em	171 ± (1.8)	−358 ± (2.3)	−19 ± (1.8)
EI	238 ± (1.8)	−354 ± (2.3)	−19 ± (1.8)

[a]AC is expressed in the local coordinate system of the scapula.

Palpation error E_P

The effect of the standard deviation σ_q (Table 4) of the skeletal landmarks on the positions of the bones expressed in Cardan angles $\leq_x$ was estimated by Equation 2, using the fifth-order polynomials (Figure 3). The average results are represented by the first bar of each interval (Figure 5). The second and third bars represent the intra- and inter-individual standard deviations, respectively.

Motoric noise E_M and inter-subject variability E_S

The variance of independent variables, defined by the squared standard deviations add linearly (Equations 3 and 4). As E_P, σ_{intra} and σ_{inter} are known variables, the E_M and E_S can be derived from Equations 3 and 4, respectively. The three independent sources of variation have been expressed as a percentage of the σ^2_{inter} for the total range of arm abduction (Table 5). The contribution of each of the independent factors to the inter-individual standard deviation is shown in Figure 6.

Scapular coordinate system (AA versus AC)

The decomposition of rotation matrices to Cardan angles is singular at the gimbal lock position, resulting in an increasing inaccuracy near this position. This is illustrated by the relatively high standard error of the humerus rotation angles (y and y'') at the first and fourth abduction interval. The same interaction between the (y and x'') angles may appear at maximal latero-rotation of the scapula. Using AA to define the local x_s-axis this is hardly the case (Figure 5). If the AC landmark is used instead, however, the inaccuracy increases remarkably (Figure 7). Near maximal arm abduction the latero-rotation reaches 90°. The axis of protraction (y-rotation) and the axis of spinal tilt (x''-rotation) are more or less aligned in this position. Both rotations therefore describe more or less the same rotation. The first column of Figure 7 shows that positive deviations of the average protraction are counteracted by negative spinal tilt and vice versa. This dispersion, quantified by the standard deviation (Figure 7, second column) increases drastically at the fourth interval.

Discussion

The individual and overall movement patterns have been presented, expressed in Cardan angles with the standard errors. The results depend on the choice of the local coordinate system, based on the skeletal landmarks and the order of the Cardan angles by which the rotations are parameterized. At first, and in the perspective of standardization of coordinate systems of the shoulder[15], the choice of the local coordinate system of the scapula is discussed. Subse-

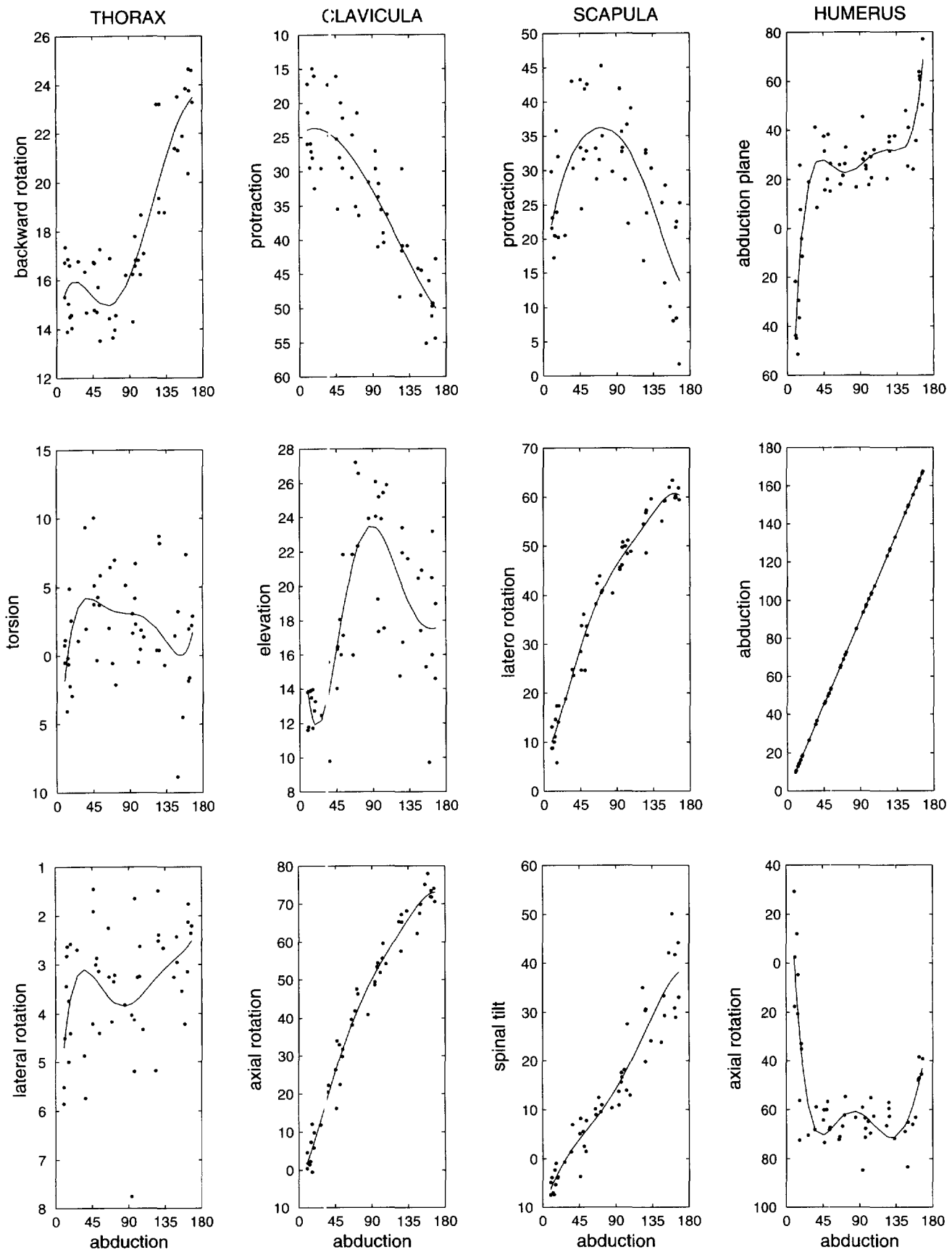

Figure 3. Fifth-order polynomial least squares fit (bold lines) of the Cardan angles of the shoulder bones during humerus abduction in the scapular plane based on the 50 individual position registrations of a single subject (dots). The three Cardan angles, describing the rotations of a single bone, are vertically represented according to the definitions of Table 3.

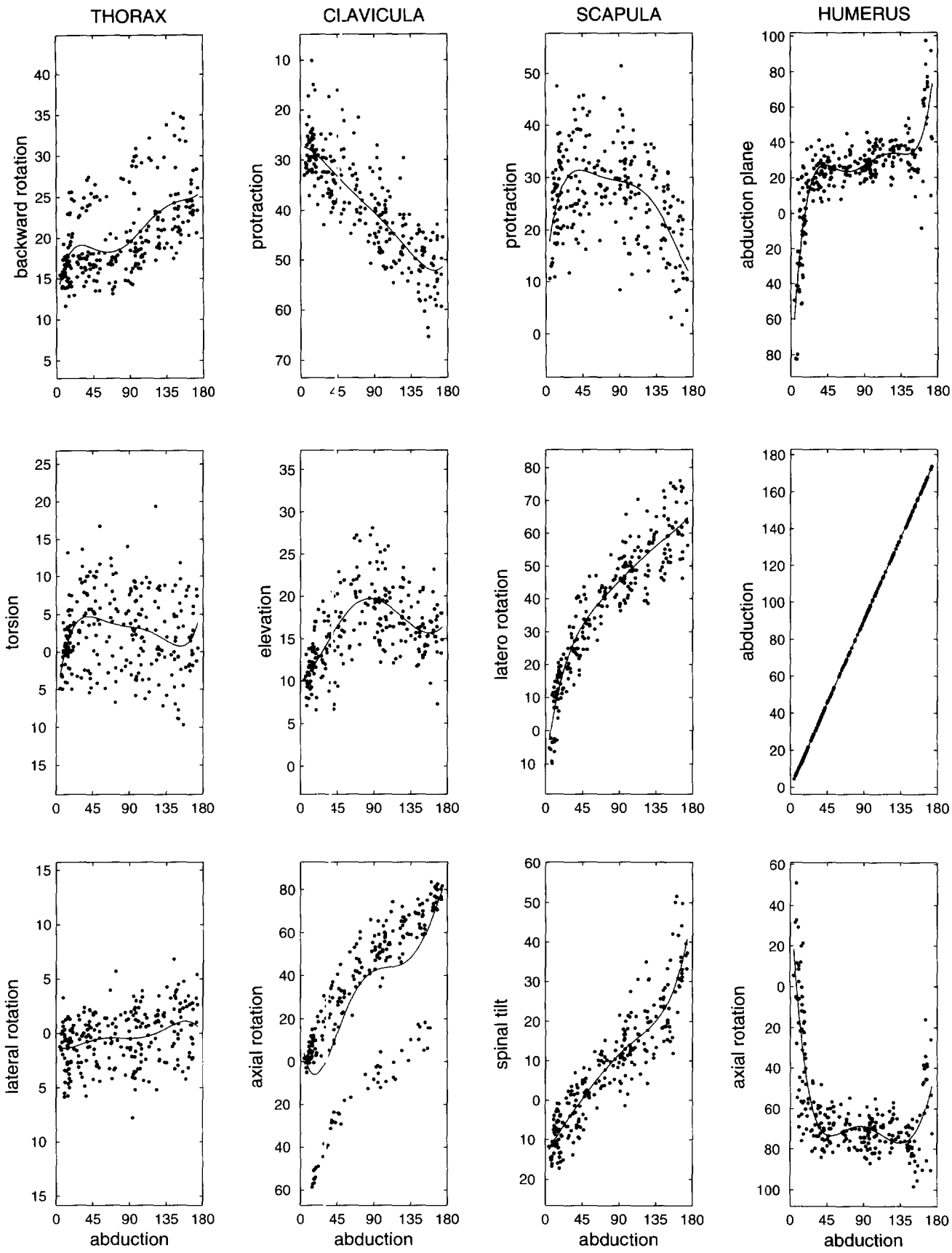

Figure 4. Fifth-order polynomial least squares fit (bold lines) of the Cardan angles of the shoulder bones during humerus abduction in the scapular plane based on the 250 position registrations of $N_S = 5$ subjects (dots). Each of the three angles are represented vertically according to the definitions of Table 3.

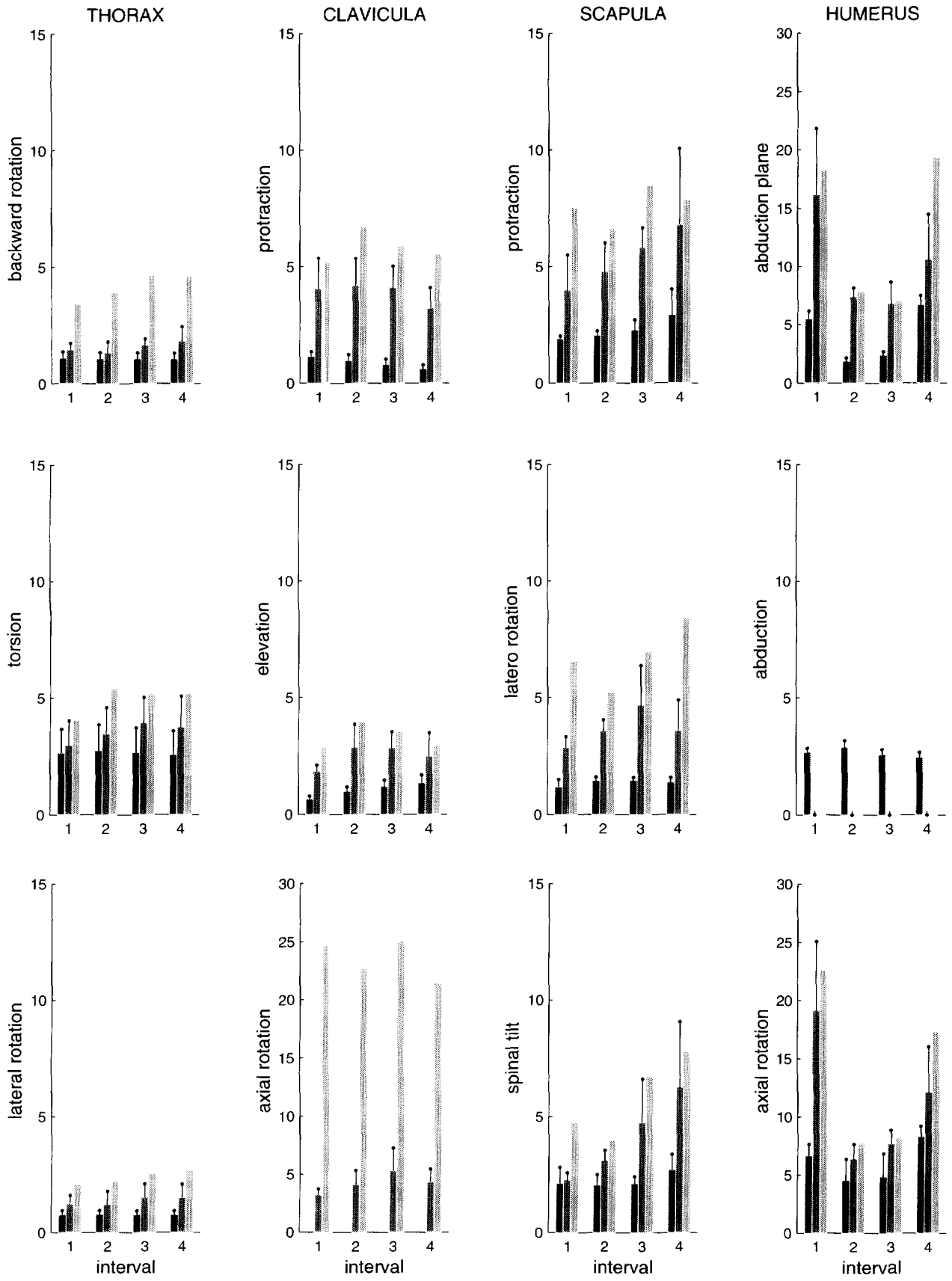

σ_{palp}, inaccuracy due to errors in the palpated positions of the skeletal landmarks.
σ_{intra}, intra-individual variability of the movement.
σ_{inter}, inter-individual variability of the movement.

Figure 5.

quently, the independent factors that determine the observed variability of the Cardan angles are discussed. Finally, the results are evaluated with respect to the possible applications of the method.

Definition of the local axes

In describing shoulder motions, different definitions of coordinate systems have been discussed[1,3,6]. Efforts are being made to standardize the orientation of the local coordinate systems and definitions of rotation[15]. The definitions used here to calculate the coordinate system of the scapula (Table 2) have been used previously[3,5]. The definitions are chosen so that the X_S, Y_S-plane is parallel to the scapular plane and the X_S-axis is aligned with the spinal ridge (TS, AA). Although using the AC landmark would facilitate the estimation of the relative rotations in the AC, the latero-rotation is increased by approximately 10°. At maximal arm abduction this results in an increase in the interaction between the first and third rotations (gimbal-lock singularity).

The movements of the scapula here are expressed in the global coordinate system. The position is the result of the relative position with respect to the thorax and the global position of the thorax. At maximal arm abduction positions, part of the backward rotation of the thorax is added to the (global) latero-rotation of the scapula. By means of the description of the relative movements of the scapula with respect to the thorax[6,7], the latero-rotation of the scapula would be reduced but would still be subject to singularity inaccuracy.

It is concluded that the defenitions based on the AA, instead of the AC[3,5] are preferred. The motions should be defined with respect to a unique reference orientation aligned with the global coordinate system of the thorax[6].

NOTE: In order to remain compatible with other authors, to be able to link the clavicle and the scapula, to estimate the position of the GH joint[11] (Appendix), and to be able to calculate global (AC and GH) joint rotations[7,15] the position of the AC landmark must always be defined in the scapular

Table 5. Standard deviation of palpation (σ_P), motoric noise (σ_M) and morphology (σ_S) for each of the cardanic rotations at each bony element expressed by the percentage of the inter-individual variance σ_{inter}

	σ_P (%)	σ_M (%)	σ_S (%)
Thorax			
Backward rotation	6	9	85
Torsion	40	13	48
Lateral rotation	14	16	70
Clavicula			
Protraction	2	36	62
Elevation	11	45	44
Axial rotation[a]	–	(41)	(59)
Scapula			
Protraction	11	42	48
Latero-rotation	4	25	71
Spinal tilt	15	38	47
Humerus			
Abduction plane	8	54	38
Elevation	–	–	–
Axial rotation	14	55	31

[a]The axial rotations of the clavicula not measured but derived by minimization of the rotations in the AC joint [6].

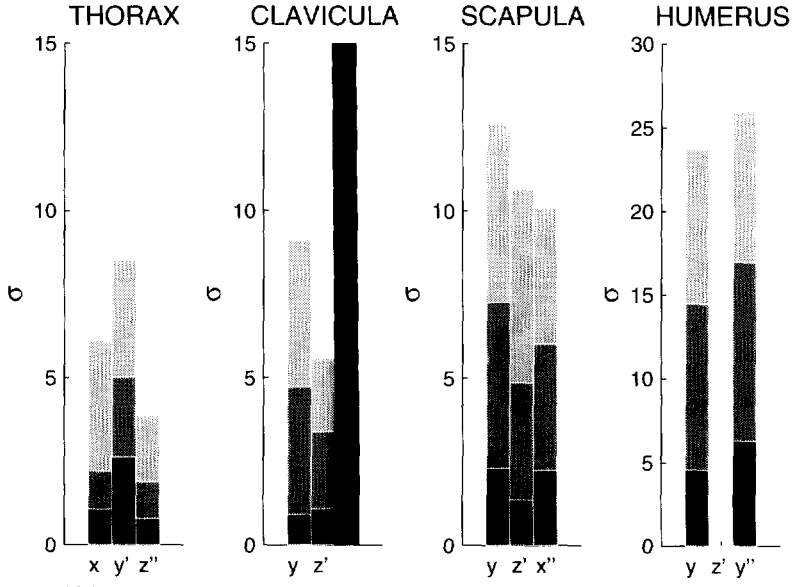

contribution of the palpation error (E_P)
contribution of the motoric noise (E_M)
contribution of the inter-subject variability (E_S)

(the axial rotation of the clavicula is left out as it not a measured but a derived quantity).
Figure 6.

coordinate system, together with the AA, TS and AI landmarks.

Variability of shoulder postures

The shoulder positions are parameterized by means of Cardan angles. A fifth-order curve fitting is applied. The high order was chosen in order to be able to describe the sharp curves of the first and third humerus rotations (Y_H, Y_H'').

The humerus position of the subject was the task variable. During the mid-range elevation the task is well defined (Figure 3 and Figure 4), with a constant abduction plane ($\approx 30°$) and axial rotation ($\approx 75°$). Near minimal and maximal arm abduction, the abduction plane parameter and the axial rotation parameter interfere with each other as the positions are close to the singular positions in the Cardan decomposition (Y_H, Z_H', Y_H'').

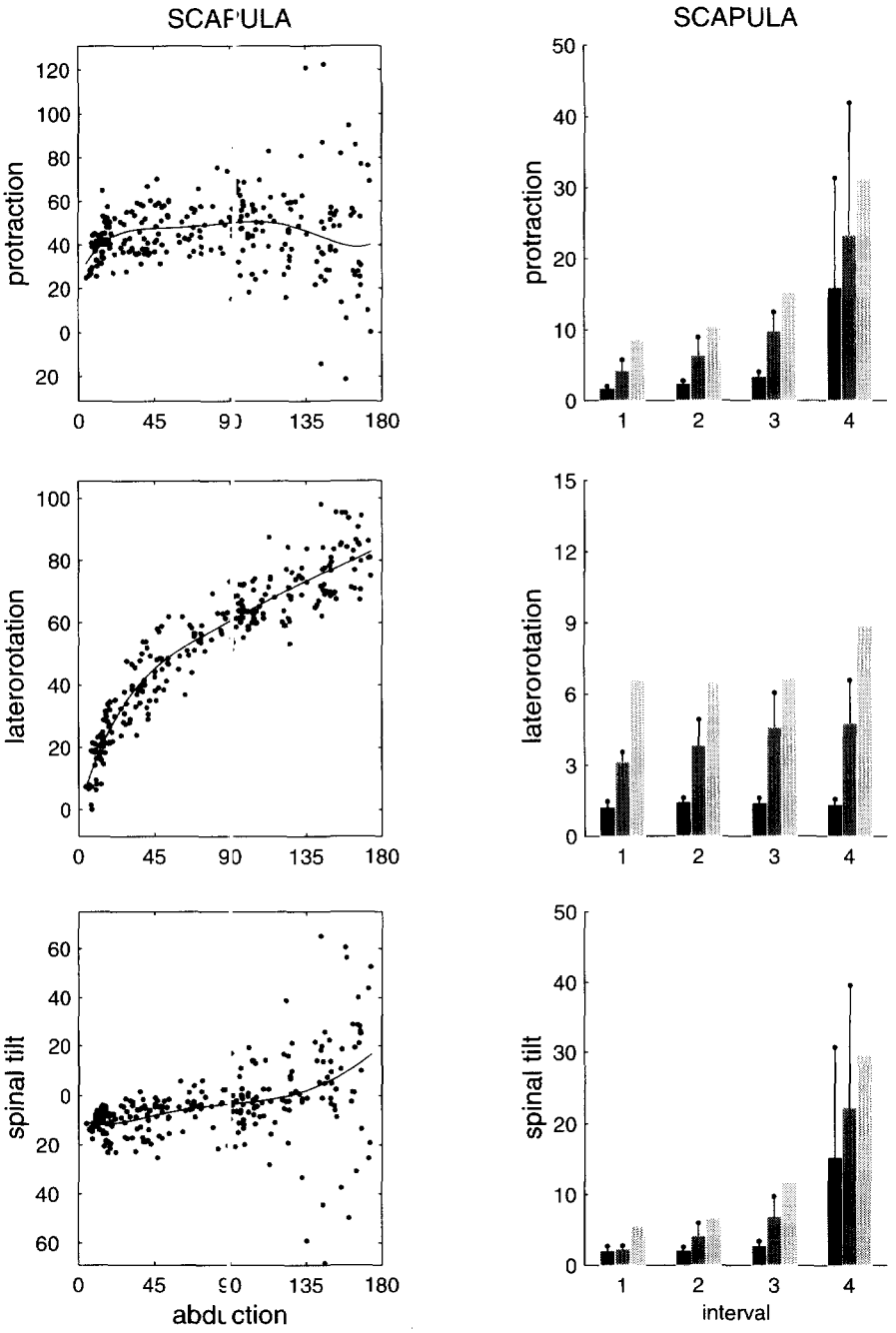

σ_{palp}, inaccuracy due to errors in the palpated positions of the skeletal landmarks.
σ_{intra}, intra-individual variability of the movement.
σ_{inter}, inter-individual variability of the movement.

Figure 7.

The E_P was determined based on the palpation error of the skeletal landmarks. Except for the humerus the E_P is constant for the different abduction intervals, indicating that non-linear effects due to Cardan decomposition are small. As a result of the addition of independent variability sources (E_P, E_M and E_S), the variance increases in the order of palpation error, intra-individual variance and inter-individual variance. The contribution of E_P in the total inter-individual variance is the lowest ($12 \pm 10\%$) with an absolute value of less than 3°, except for the axial rotation of the humerus. This is equal to the estimated value, based on homogeneous palpation variance distribution on the skeletal landmarks[6].

The existence of E_M means that the kinematic relationship of the humerus with respect to the thorax, clavicula and scapula is not unique. Less than half of the inter-individual variance ($33 \pm 17\%$) originates from this kinematic redundancy. This motor noise was also found with dynamic two-dimensional (2D) Roentgen video recordings[8].

The magnitude of the intra-individual standard deviation reported by Johnson et al.[5] was less than 2°. Some accuracy might have been gained from their method of position registration which might have reduced the E_P, but this cannot explain the reduction of the motor noise.

The major source of variability is the inter-subject variability E_S of ($55 \pm 16\%$). The order of magnitude is equal to the data of Pronk[3] (5–10°). The most obvious cause of this variability is the morphological difference between the subjects. A way of reducing this variability is to choose the initial position as a reference position to express the rotations, instead of the reference orientation being aligned with the global coordinate system, as used here. The rotations would become relative parameters, and information about the global movement would be lost.

Application of palpation for 3D movement descriptions

The 3D movement of the scapula cannot be recorded from fixed skin markers. Palpation and subsequent digitizing is a non-invasive alternative. On the basis of the palpation error and the intra- and inter-individual variance, the validity of the palpation method can be estimated.

The palpation error is approximately 2° (Figure 5). With $N_1 = 5$ recordings the 95% confidence interval of the mean (CI) is approximately 2.5°. A two-tailed t-test ($P = 0.05$) would indicate a significant difference between populations if the means of two samples ($N = 5$) differ by $3E$ or more.

Because of the large amplitude and the equivalence with the 2D scapulohumeral rhythm, the latero-rotation of the scapula with respect to the humerus abduction is an intra-individual parameter of clinical importance. This parameter can be used to express the pre- and post-treatment kinematics of frozen shoulder, impingement, GH endoprosthesis or the success of GH arthrodesis. If two sets of recordings of five measurements each are compared, e.g. pre- and post-treatment recordings of the same patient, the CI is equal to 5° and a difference of 5.9° or more would indicate a significant difference (for $N = 5$, $P_{2\text{-tailed}} = 0.05$, $\sigma_{intra} = 4°$). The method can be made more discriminative by increasing the number of observations.

The latero-rotation of the scapula might also be used to identify groups of patients with shoulder disorders. With a $\sigma_{inter} = 6°$ a significant difference between two groups of $N = 5$ subjects is found at 8.8° or more. However, with respect to the maximal latero-rotation of 60°, a distinction level of 15% is rather large. The resolution can be increased by increasing the number of samples (e.g. a distinction level of 5° at $N = 13$), but it will not be possible to discriminate a single patient from a normal group within a reasonably small resolution.

Conclusions

The palpation method is a powerful and accurate tool for recording the 3D kinematics of the thorax, the humerus and especially the clavicula and the scapula. As large skin displacements occur during movement with respect to the latter bones optical methods with fixed skin markers are not appropriate.

The accuracy of the angular Cardan parameters is sensitive for the definition of the local coordinate systems and the order of rotation. For the scapula the coordinate system, based on the skeletal landmarks AA, TS and AI and expressed in the global reference system, is less sensitive for singular positions than the coordinate system based on the AC, TS and AI.

The palpation error E_P is small, and results in a relatively small contribution (<3°) to the inter-individual variance of the Cardan parameters, which are also influenced by motoric noise E_M (3–6°) and inter-subject variability E_S (5–10°).

The method can be very useful in follow-up of the treatment of patients with shoulder disorders involving kinematic deviations. The method can also be used to identify groups of patients with specific shoulder disorders, but the identification of a single patient with respect to a normal group will be very hard, because of the large inter-subject variability E_S.

Appendix

Glenohumeral landmark regression algorithm[11]

The GH landmark is essential in the definition of the local coordinate system of the humerus. This skeletal landmark is difficult to locate *in vivo*. It is assumed that the rotation centre is fixed both with respect to the humerus and the scapula. The position can be

deduced from a regression equation based on the skeletal landmarks of the scapula: the AC, AA, TS and AI. The equation is based on the data of 14 left and right scapula specimens.

Algorithm

Determination of the right-handed local coordinate system R_S: (X_S, Y_S, Z_S) and O_S of the scapula based on the recorded coordinates (mm) of the skeletal landmarks AA, AC, TS and AI, Equations 1a–d:

$$X-\text{axis: } X_S = (AC-TS)/|(AC-TS)| \quad (A.1a)$$

$$Y-\text{axis: } Y_S \text{ perpendicular to the plane } AC-TS-AI \quad (A.1b)$$

$$Z-\text{axis: } Z_S \text{ perpendicular to } X_S \text{ and } Y_S \quad (A.1c)$$

$$\text{Origin: } O_S = (AC+AA)/2 \quad (A.1d)$$

Determination of the landmarks in the local coordinate system, Equations 2a, 2b, 2c and 2d:

$$ac = R_S^{Inv}.\ (AC-O_S) \quad (A.2a)$$

$$aa = R_S^{Inv}.\ (AA-O_S) \quad (A.2b)$$

$$ts = R_S^{Inv}.\ (TS-O_S) \quad (A.2c)$$

$$ai = R_S^{Inv}.\ (AI-O_S) \quad (A.2d)$$

Determination of the distances between the landmarks used in the regression equation, Equations (3a and b):

$$L_{acts} = |ac-ts| \quad (A.3a)$$

$$L_{acai} = |ac-ai| \quad (A.3b)$$

Calculation of the position of the GH rotation centre in the local coordinate system of the scapula, Equation 4:

$$gh = \begin{vmatrix} 1 & L_{acts} & L_{acai} \\ 1 & L_{acts} & L_{acai} \\ 1 & L_{acts} & L_{acai} \end{vmatrix} \cdot \begin{vmatrix} 10 & -70 & -3 \\ -40 & 0.73 & -0.30 \\ 0.22 & -0.28 & 0.06 \end{vmatrix} \quad (A.4)$$

Repositioning of the local defined GH rotation centre in the global coordinate system, Equation 5:

$$GH = R_S \cdot gh + O_S \quad (A.5)$$

References

1. Högfors, C., Sigholm, G. and Herberts, P. Biomechanical model of the shoulder — I: elements. *Journal of Biomechanics*, 1991, **20**, 157–166.
2. Harryman, D. T., Sidles, J. A., Harris, S. L. and Matsen, F. A. Laxity of a normal glenohumeral joint: a quantitative *in vivo* assessment. *Journal of Shoulder and Elbow Surgery*, 1991, **1**, 66–76.
3. Pronk, G. M., The shoulder girdle. Ph.D. thesis, University of Delft, The Netherlands, ISBN 90-370-0053-3, 1991.
4. Pronk, G. M. and Van der Helm, F. C. T. The palpator, an instrument for measuring the three-dimensional positions of bony landmarks in a fast and easy way. *Journal of Medical Engineering and Technology*, 1991, **15**, 15–21.
5. Johnson, G. R., Stuart, P. R. and Mitchell, S. A method for the measurement of three-dimensional scapular movement. *Journal of Clinical Biomechanics*, 1993, **8**, 269–273.
6. Van der Helm, F. C. T. Analysis of the kinematic and dynamic behaviour of the shoulder mechanism. *Journal of Biomechanics*, 1994, **27**, 527–550.
7. Van der Helm, F. C. T. and Pronk, G. M. Three-dimensional recording and description of motions of the shoulder mechanism. *Journal of Biomechanical Engineering*, 1995, **177**, 27–40.
8. De Groot, J. H., Valstar, E. R., Arwert, H. J., Velocity effects on the scapulo-humeral rhythm. Submitted to Journal of Clinical Biomechanics, 1995.
9. Soslowski, L. J., Ateshian, G. A., Mow, V. C., Stereophotogrammetric determination of joint anatomy and contact areas. Biomechanics of diarthrodial joints. Volume eds. V. C. Mow, A. Ratcliffe and S. L.-Y. Woo, 1990.
10. Van der Helm, F. C. T., Pronk, G. M., Veeger, H. E. J., Van der Woude, L. H. V. and Rozendal, R. H. Geometry parameters for musculoskeletal modelling of the shoulder mechanism. *Journal of Biomechanics*, 1992, **25**, 129–144.
11. Rozendaal, L. Estimation of the position of the centre of rotation of the glenohumeral joint from skeletal landmarks of the scapula. 1997, in prep.
12. Runciman, R. J. and Nicol, A. C. Modelling muscle and joint forces at the gleno-humeral joint: an overview of a current study (Journal of Engineering in Medicine) (ImechE). *Proceedings Instrumentation of Mechanical Engineering*, 1994, **207**, 229–291.
13. Woltring, H. J. Representation and calculation of 3-D joint movement. *Human Movement Sciences*, 1991, **10**, 603–616.
14. Jenkins, G. M., Watts, D. G., *Spectral Analysis and its Applications*. Holden–Day, 1969.
15. Van der Helm, F. C. T., Joints of the shoulder mechanism: definition of joint coordinate systems, joint motions and joint torques. Submitted to Journal of Biomechanics, 1995.